

2014

# Development and intrinsic properties of hexagonal ferromagnetic (Zr,Ti)Fe<sub>2</sub>

Wenyong Zhang

University of Nebraska-Lincoln, wenyong.zhang@unl.edu

Xingzhong Li

University of Nebraska-Lincoln, xli2@unl.edu

Shah R. Valloppilly

University of Nebraska-Lincoln, svalloppilly2@unl.edu

Ralph A. Skomski

University of Nebraska-Lincoln, rskomski2@unl.edu

Jeffrey E. Shield

University of Nebraska-Lincoln, jshield@unl.edu

*See next page for additional authors*

Follow this and additional works at: <http://digitalcommons.unl.edu/physicsellmyer>

 Part of the [Physics Commons](#)

---

Zhang, Wenyong; Li, Xingzhong; Valloppilly, Shah R.; Skomski, Ralph A.; Shield, Jeffrey E.; and Sellmyer, David J., "Development and intrinsic properties of hexagonal ferromagnetic (Zr,Ti)Fe<sub>2</sub>" (2014). *David Sellmyer Publications*. 260.

<http://digitalcommons.unl.edu/physicsellmyer/260>

This Article is brought to you for free and open access by the Research Papers in Physics and Astronomy at DigitalCommons@University of Nebraska - Lincoln. It has been accepted for inclusion in David Sellmyer Publications by an authorized administrator of DigitalCommons@University of Nebraska - Lincoln.

---

**Authors**

Wenyong Zhang, Xingzhong Li, Shah R. Valloppilly, Ralph A. Skomski, Jeffrey E. Shield, and David J. Sellmyer

## Development and intrinsic properties of hexagonal ferromagnetic (Zr,Ti)Fe<sub>2</sub>

W. Y. Zhang,<sup>1,2,a)</sup> X. Z. Li,<sup>1</sup> S. Valloppilly,<sup>1</sup> R. Skomski,<sup>1,2</sup> J. E. Shield,<sup>1,3</sup>  
 and D. J. Sellmyer<sup>1,2</sup>

<sup>1</sup>Nebraska Center for Materials and Nanoscience, University of Nebraska, Lincoln, Nebraska 68588, USA

<sup>2</sup>Department of Physics and Astronomy, University of Nebraska, Lincoln, Nebraska 68588, USA

<sup>3</sup>Department of Mechanical and Materials Engineering, University of Nebraska, Lincoln, Nebraska 68588, USA

(Presented 6 November 2013; received 23 September 2013; accepted 19 December 2013; published online 26 March 2014)

Nanocrystalline Ti<sub>0.75</sub>Zr<sub>0.25</sub>Fe<sub>2+x</sub> ( $x = 0-0.4$ ) and Ti<sub>0.75-y</sub>B<sub>y</sub>Zr<sub>0.25</sub>Fe<sub>2.4</sub> ( $y = 0-0.35$ ) with high saturation magnetization have been fabricated by the melt-spinning technique. Nanocrystalline Ti<sub>0.75</sub>Zr<sub>0.25</sub>Fe<sub>2+x</sub> consists of the hexagonal C14 Laves phase (Ti,Zr)Fe<sub>2</sub>. Fe addition decreases the lattice parameter  $a$  and shrinks the cell volume. The antiferromagnetic Fe-Fe interactions may decrease with the increase of  $x$ , leading to a significant enhancement of saturation polarization ( $J_s$ ) and Curie temperature ( $T_c$ ). The magnetocrystalline anisotropy constant  $K$  also increases with increasing  $x$ . Excessive Fe addition ( $x > 0.25$ ) may induce structural disorder which lowers the  $J_s$  and  $T_c$ . Nanocrystalline Ti<sub>0.75-y</sub>B<sub>y</sub>Zr<sub>0.25</sub>Fe<sub>2.4</sub> is composed of hexagonal (Ti,Zr)Fe<sub>2</sub> and Fe-rich amorphous phases with relatively high  $J_s$ . The lattice parameters  $a$ ,  $c$  and cell volume  $V$  are almost unchanged with the increase of  $y$  for  $y \geq 0.16$ . Simultaneously, the  $T_c$  of (Ti,Zr)Fe<sub>2</sub> remains unchanged, indicating that B does not enter this lattice but takes part in forming the amorphous phase, in good agreement with the X-ray diffraction results. The volume fraction of the amorphous phase increases with the increase of B content and results in a large enhancement of  $J_s$  up to 10.8 kG. Further B addition ( $y > 0.30$ ) decreases  $J_s$ , possibly due to the decrease of the  $J_s$  of the amorphous phase. © 2014 AIP Publishing LLC. [<http://dx.doi.org/10.1063/1.4868696>]

The magnetic properties of the C14 Laves phase TiFe<sub>2</sub> with the hexagonal structure show strong composition dependence due to the existence of the energetic near-degeneracy of an antiferromagnetic (AF) and ferromagnetic (FM) ground state.<sup>1,2</sup> The Ti-Fe alloy has a wide homogeneity range at 1300 °C,<sup>3,4</sup> leading to the appearance of a composition variation at room temperature for TiFe<sub>2</sub>. Between  $x = 0$  and  $x = 0.7$ , TiFe<sub>2+x</sub> may be AF and FM.<sup>5,6</sup> Stoichiometric TiFe<sub>2</sub> is AF, while Fe-rich TiFe<sub>2</sub> shows FM. So far, much work has been done on how the alloy composition affects basic magnetism of microcrystalline Ti-Fe alloys. Little attention has been paid to studying the effect of element addition on nanostructure and intrinsic properties of nanocrystalline Ti-Fe. A high quench rate is favorable to keep the high-temperature metastable phase to room temperature. In this work, we added 25 at. % Zr in order to decrease the fraction of AF alignment of intralayer Fe. We fabricated nanocrystalline Zr<sub>0.25</sub>Ti<sub>0.75</sub>Fe<sub>2+x</sub> ( $x = 0-0.4$ ) and Zr<sub>0.25</sub>Ti<sub>0.75-y</sub>B<sub>y</sub>Fe<sub>2.25</sub> ( $y = 0-0.16$ ) by melt spinning and investigate the effects of Fe and B content on intrinsic properties. All the samples exhibit FM. Fe and B additions lead to a large improvement of Curie temperature and saturation magnetization.

Ingots of Ti<sub>0.75</sub>Zr<sub>0.25</sub>Fe<sub>2+x</sub> ( $x = 0, 0.15, 0.25, 0.40$ ) and Ti<sub>0.75-y</sub>B<sub>y</sub>Zr<sub>0.25</sub>Fe<sub>2.4</sub> ( $y = 0, 0.16, 0.30, 0.35$ ) were arc melted from high-purity elements in an argon atmosphere. The ribbons were made by ejecting molten alloys in a quartz tube onto the surface of a copper wheel with a speed of

15 m/s. The ribbons are about 2 mm wide and 50 μm thick. The phase components were examined by Rigaku D/Max-B X-ray diffraction (XRD) with Co K<sub>α</sub> radiation. The nanostructure was observed by the Tecnai Osiris Transmission Electron Microscope (TEM). The hysteresis loops were measured by a superconducting quantum interference device (SQUID) magnetometer at fields up to 7 T. Intrinsic properties: saturation magnetization, magnetocrystalline anisotropy constant, anisotropy field were determined by fitting the high-field part of hysteresis loops using the law-of-approach to saturation. Thermomagnetic curves were obtained using a Physical Property Measurement System (PPMS) vibrating sample magnetometer (VSM). The applied field is parallel to the long direction of the ribbon.

Figures 1(a) and 1(b) show XRD patterns of nanocrystalline Ti<sub>0.75</sub>Zr<sub>0.25</sub>Fe<sub>2+x</sub> ( $x = 0, 0.40$ ) and Ti<sub>0.75-y</sub>B<sub>y</sub>Zr<sub>0.25</sub>Fe<sub>2.4</sub> ( $y = 0.16, 0.30$ ). All the diffraction peaks were indexed to the hexagonal C14 structure. The Ti<sub>0.75</sub>Zr<sub>0.25</sub>Fe<sub>2+x</sub> consists of the C14 structure except that here is an obvious shift of diffraction peaks for the Ti<sub>0.75</sub>Zr<sub>0.25</sub>Fe<sub>2+x</sub> due to Fe addition. This implies a change of lattice parameters. The diffraction peaks for the Ti<sub>0.75-y</sub>B<sub>y</sub>Zr<sub>0.25</sub>Fe<sub>2.4</sub> did not shift, indicating that the lattice parameters remain unchanged. A halo peak between 35° and 55° appears in the Ti<sub>0.75-y</sub>B<sub>y</sub>Zr<sub>0.25</sub>Fe<sub>2.4</sub>, implying the existence of an amorphous phase. The relative intensity of the halo peak increases with the increase of B content suggesting that the volume fraction of the amorphous phase increases with increasing  $y$ . The Ti<sub>0.75-y</sub>B<sub>y</sub>Zr<sub>0.25</sub>Fe<sub>2.4</sub> is composed of the crystalline (Ti,Zr)Fe<sub>2</sub> and amorphous phases. Figures 1(c) and 1(d) show B and Fe content dependence of cell

<sup>a)</sup>Author to whom correspondence should be addressed. Electronic mail: wenyong.zhang@unl.edu.

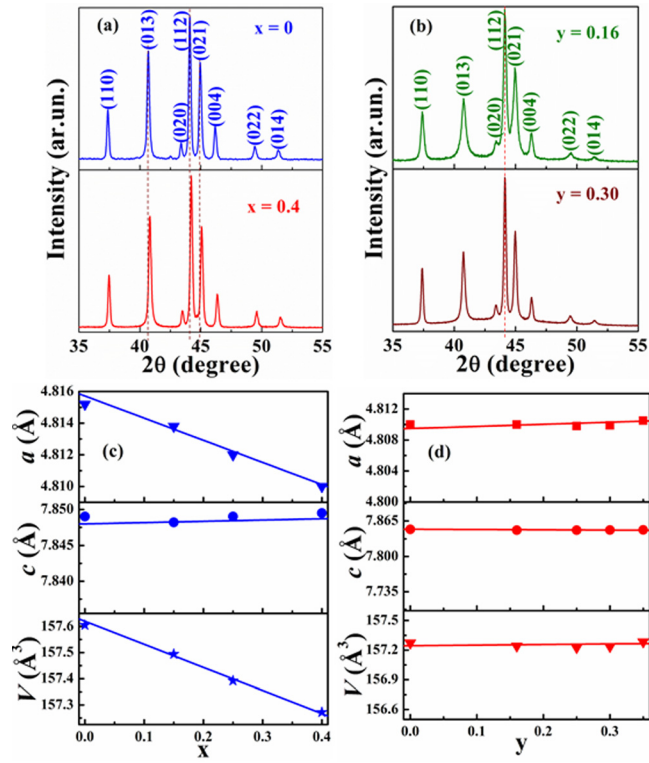


FIG. 1. XRD patterns of (a)  $\text{Ti}_{0.75}\text{Zr}_{0.25}\text{Fe}_{2+x}$  ( $x=0, 0.4$ ), (b)  $\text{Ti}_{0.75-y}\text{B}_y\text{Zr}_{0.25}\text{Fe}_{2.4}$  ( $y=0.16, 0.30$ ). And corresponding (c)  $x$  and (d)  $y$  dependence of cell parameters ( $a, c, V$ ).

parameters ( $a, c, V$ ). Fe addition leads to no change of  $c$ , a decrease of  $a$ , and thus a decrease of  $V$ . It is believed that extra Fe ( $R_{\text{Fe}}=126\text{ pm}$ ) replaces some amount of Ti ( $R_{\text{Ti}}=147\text{ pm}$ ) or Zr ( $R_{\text{Zr}}=160\text{ pm}$ ), leading to the shrinkage of the cell volume. Occupancy site of extra Fe needs to be further investigated. B addition results in a slight increase of  $a, c, V$  of the crystalline phase. The lattice parameters of the crystalline phase are almost unchanged with  $y$  and close to those of the  $x=0.25$  shown in Fig. 1(c). The composition of the crystalline phase is presumably  $\text{Ti}_{0.75}\text{Zr}_{0.25}\text{Fe}_{2.25}$ .

Figure 2 shows thermomagnetic curves for the  $x=0, 0.25$  and  $y=0.30$ . The Curie temperature ( $T_c$ ) was determined from the peak position of the  $dM/dT$  vs  $T$  plot shown in the inset. The  $M(T)$  curves of the  $x=0$  and  $0.25$  only have one ferro-paramagnetic transition from the magnetic (Ti,Zr)Fe<sub>2</sub>. TiFe<sub>2</sub> is an antiferromagnet with  $T_N=270\text{ K}$ .<sup>7</sup> Replacement

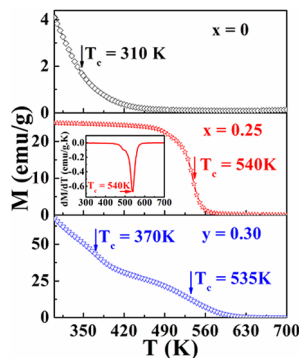


FIG. 2.  $M(T)$  curves of  $\text{Ti}_{0.75}\text{Zr}_{0.25}\text{Fe}_{2+x}$  ( $x=0, 0.25$ ) and  $\text{Ti}_{0.75-y}\text{B}_y\text{Zr}_{0.25}\text{Fe}_{2.4}$  ( $y=0.30$ ).

of Ti by Zr to form  $\text{Ti}_{0.75}\text{Zr}_{0.25}\text{Fe}_2$  yields a ferromagnet with  $T_c=315\text{ K}$ . This trend is consistent with the ferromagnetism of the nearly isostructural (C15) laves phase  $\text{ZrFe}_2$ . Addition of excess Fe to form  $\text{Ti}_{0.75}\text{Zr}_{0.25}\text{Fe}_{2.25}$  also increases  $T_c$  to  $540\text{ K}$ . This is likely the result of increased number of ferromagnetic Fe-Fe bonds. There are two ferro-paramagnetic transitions in the  $M(T)$  curves of the  $y=0.30$  which correspond to the amorphous and crystalline phases. The  $T_c$  of the crystalline phase is almost the same as that for  $x=0.25$  which is consistent with a composition of the crystalline phase being  $\text{Ti}_{0.75}\text{Zr}_{0.25}\text{Fe}_{2.25}$ .

Figure 3 shows the TEM images of the  $x=0.25, 0.40$  and  $y=0.30$  samples. The nanostructure exhibits strong dependence on alloy composition. The composition of the grains for  $x=0.25$  and  $0.40$  checked by Energy-dispersive X-ray spectroscopy (EDX) are close to  $\text{Ti}_{0.75}\text{Zr}_{0.25}\text{Fe}_{2.25}$  and  $\text{Ti}_{0.75}\text{Zr}_{0.25}\text{Fe}_{2.4}$ , respectively. The mean grain size for  $x=0.25$  is much larger than that for  $x=0.40$ . Excessive Fe addition induces the appearance of many bands indicated by red arrows. High-resolution images (not shown here) show that they are planar defects. The TEM image of the  $y=0.30$  sample consists of grains and gray area indicated by yellow circles corresponding to the amorphous phase. No B was detected in the grains of the  $x=0.30$  sample. It was estimated that the composition of the amorphous phase for  $y=0.30$  is  $\text{Zr}_{0.25}\text{B}_{0.75}\text{Fe}_{2.63}$  and its concentration is 40 at. %. The concentrations of the amorphous phase for  $y=0.16$  and  $0.35$  are 21.3 and 47 at. %, respectively. The B content and amorphous phase increase are consistent with the XRD results.

Figure 4 shows typical hysteresis loops of nanocrystalline  $\text{Ti}_{0.75}\text{Zr}_{0.25}\text{Fe}_{2+x}$  ( $x=0-0.4$ ) and  $\text{Ti}_{0.75-y}\text{B}_y\text{Zr}_{0.25}\text{Fe}_{2.4}$  ( $y=0-0.35$ ) and deduced intrinsic properties. Fe addition increases  $J_s$  and  $T_c$  possibly due to the decrease of AF Fe-Fe interactions. Excessive Fe addition may induce the formation of structural disorder including planar defects, and thus lowers  $J_s$  and  $T_c$ . The  $K$  value increases first, which may be related to the decrease of lattice parameter  $a$ . Up to a maximum value at  $x=0.15$ , and then slightly decreases possibly due to the increase of structural disorder such as planar defects. B addition leads to the formation of a large amount of amorphous phase which may have a high saturation

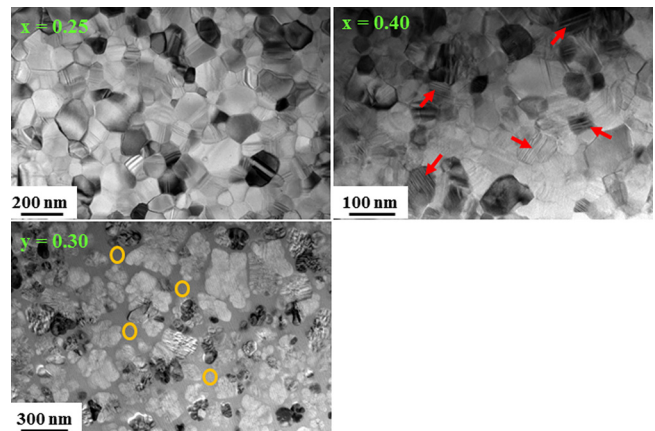


FIG. 3. TEM images of  $\text{Ti}_{0.75}\text{Zr}_{0.25}\text{Fe}_{2+x}$  ( $x=0.25, 0.40$ ) and  $\text{Ti}_{0.75-y}\text{B}_y\text{Zr}_{0.25}\text{Fe}_{2.4}$  ( $y=0.30$ ).

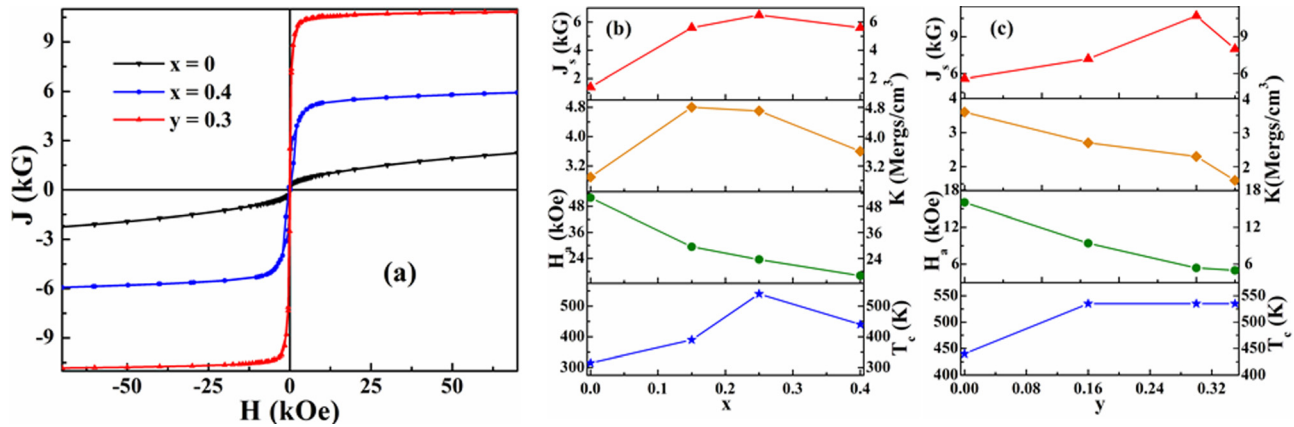


FIG. 4. Hysteresis loops of  $\text{Ti}_{0.75}\text{Zr}_{0.25}\text{Fe}_{2+x}$  ( $x=0, 0.4$ ) and  $\text{Ti}_{0.75-y}\text{B}_y\text{Zr}_{0.25}\text{Fe}_{2.4}$  ( $y=0.30$ ) (a). And  $x$  (b) and  $y$  (c) dependence of deduced intrinsic properties ( $J_s$ ,  $K$ ,  $H_a$ , and  $T_c$ ).

magnetization. Therefore,  $J_s$  of the  $\text{Ti}_{0.75-y}\text{B}_y\text{Zr}_{0.25}\text{Fe}_{2.4}$  increases rapidly with the increase of B content.  $K$  decreases continuously with  $y$  due to the formation of soft magnetic amorphous phase. The  $T_c$  of the crystalline phase is independent of B content, indicating B hardly enters the crystalline phase. Further B addition ( $y > 0.30$ ) results in a decrease of  $J_s$  due possibly to the decrease of magnetization of the amorphous phase. The magnetocrystalline anisotropy field of the  $(\text{Ti,Zr})\text{Fe}_2$  decreases with the increase of Fe or B content because of the big increase of saturation magnetization.

Strongly ferromagnetic  $(\text{Ti,Zr})\text{Fe}_2$  with high  $T_c$  has been synthesized. The cell volume  $V$  of the  $(\text{Ti,Zr})\text{Fe}_2$  decreases with increasing  $x$ . Fe addition significantly increases  $J_s$ ,  $T_c$ , and slightly decreases  $K$ ,  $H_a$ . Excessive Fe addition may induce the formation of structural disorder, which decreases  $J_s$  and  $T_c$ . The  $V$  of the  $(\text{Ti,Zr})\text{Fe}_2$  expands at first with the increase of B content, then remains unchanged. B addition increases  $J_s$ , but decreases  $K$  and  $H_a$ . The increase of  $J_s$  is

believed to arise from the increase of the content of amorphous phase with high magnetization.

This research was supported by the Arm Research Office under Grant Nos. WF911NF-09-2-0039 and WF911NF-10-2-0099. This work was carried out in part in the Central Facilities of the Nebraska Center for Materials and Nanoscience, which is supported by the Nebraska Research Initiative.

<sup>1</sup>J. Köble and M. Huth, *Phys. Rev. B* **66**, 144414 (2002).

<sup>2</sup>E. F. Wassermann, B. Rellinghaus, T. Roessel, and W. Pepperhoff, *J. Magn. Magn. Mater.* **190**, 289 (1998).

<sup>3</sup>W. Brückner, K. Kleinstück, and G. E. R. Schulze, *Phys. Status Solidi* **23**, 475 (1967).

<sup>4</sup>Y. Murakami, H. Kimura, and Y. Nishimura, *The Japan Institute of Metals and Materials* **21**, 665 (1957).

<sup>5</sup>E. Piegger and R. S. Craig, *J. Chem. Phys.* **39**, 137 (1963).

<sup>6</sup>W. Brückner, R. Perthel, K. Kleinstück, and G. E. R. Schulze, *Phys. Status Solidi* **29**, 211 (1968).

<sup>7</sup>T. Nakamichi, *J. Phys. Soc. Jpn.* **25**, 1189 (1968).